ESAIM: PROCEEDINGS, November 2002, Vol.12, 12-16
M.Thiriet, Editor

SIMULATION OF ELECTROPHYSIOLOGICAL WAVES WITH AN UNSTRUCTURED FINITE ELEMENT METHOD *

Yves Bourgault[1] and Marc Ethier[1]

Abstract. Bidomain models are commonly used for studying and simulating electrophysiological waves in the cardiac tissue. Most of the time, the associated PDEs are solved using explicit finite difference methods on structured grids. We propose an implicit finite element method using unstructured grids for an anisotropic bidomain model. The impact and numerical requirements of unstructured grid methods is investigated using a test case with re-entrant waves.

Résumé. Les modèles bi-domaine sont couramment utilisés pour simuler les ondes électro-physiologiques dans le tissu cardiaque. En général, les EDP associées sont résolues par des méthodes de différences finies explicites sur des maillages structurés. Nous proposons une méthodes d'éléments finis implicites sur maillages non structurés pour résoudre un modèle bi-domaine anisotrope. L'impact d'un tel choix de méthode est analysé à l'aide d'un cas test avec ondes ré-entrantes.

Introduction

Bidomain models are commonly used for simulating electrophysiological waves in the cardiac tissue [1, 2]. Detailed dynamical system analysis are available for these models, in particular for the time evolution of the tip of re-entrant spiral waves in isotropic homogeneous media which undergoes bifurcations by varying some of the model parameters [3, 4]. These spiral waves are thought to be one of the main ingredients of the heart fibrillation.

Numerical solutions of bidomain models have been and are still an important aspect of these dynamical system studies [2, 5–7]. Typically, to obtain numerical solutions over simple domains such as squares and circles, finite difference methods on structured Cartesian grids are the obvious and general choice given their simplicity and efficiency. Unfortunately, these simple methods have somewhat restricted the ability to simulate and study electrophysiological waves in more complex geometries. There are few attempts at using unstructured grid methods based on quadrilaterals [8], the goal being then to simulate electrical waves on more realistic geometries.

The present paper proposes an unstructured grid finite element method for solving an anisotropic bidomain model. We use triangular elements, thus allowing numerical solutions on arbitrary geometries because excellent meshers are available for triangular meshes. Our goal is to be able to simulate electrophysiological waves on complex geometries, in the long term on 3-D geometries using tetrahedra-based meshes. With this paper, we first want to assess the accuracy of unstructured grid methods and their ability to simulate the fine dynamical behavior of the spiral tip before we proceed with more complex geometries.

* *This work has been supported by NSERC Operating grants and a NSERC scholarship.*

[1] Department of Mathematics and Statistics, University of Ottawa, On, Canada K1N 6N5, e-mail: **ybourg@mathstat.uottawa.ca**

Article published by EDP Sciences and available at http://www.edpsciences.org/proc or http://dx.doi.org/10.1051/proc:2002003

TABLE 1. Values of k_a and k_b as a function of e

e	k_a	k_b
0.0	3.16	1.58
0.75	2.5	2.5
0.9	2.35	3.71

1. Anisotropic Bidomain Model

Bidomain models represents the electrical potential in the intra- and extra-cellular spaces of the cardiac tissue by treating each space as a continuum and considering two dependent variables, namely the intra-cellular potential ϕ_i and the extra-cellular potential ϕ_e. The intra- and extra-cellular spaces have preferred direction of conductivities, in particular because the cardiac cells are long and thin with a specific direction of alignment.

Conductivities do not only vary from the intra- to the extra-cellular space, but the ratio of anisotropy is generally not the same in both media. As a result, it is not enough to consider the trans-membrane potential $\phi = \phi_i - \phi_e$ to model the electrical potential. As proposed by Roth [9], one also needs to consider the potential $\psi = \phi_i + k\phi_e$, with k constant. Using a single variable v to model the ion activity, the anisotropic bidomain model looks after rescaling as:

$$\frac{\partial \phi}{\partial t} = \frac{1}{\epsilon} f(\phi, v) + \Delta\phi + \frac{\alpha e}{1+\alpha(1-e)} \frac{\partial^2 \psi}{\partial x^2} \tag{1}$$

$$(2 + \alpha + \frac{1}{\alpha}) \frac{\partial^2 \psi}{\partial x^2} + (2 + \alpha(1-e) + \frac{1}{\alpha(1-e)}) \frac{\partial^2 \psi}{\partial y^2} = e(1 + \frac{1}{\alpha(1-e)}) \frac{\partial^2 \phi}{\partial y^2} \tag{2}$$

$$\frac{\partial v}{\partial t} = \epsilon(\phi + \beta - \gamma v) \tag{3}$$

where $\alpha = g_{ix}/g_{ex}$, $e = 1 - \frac{g_{ex}/g_{ey}}{g_{ix}/g_{iy}}$, g_{ix} and g_{ex} are the intra- and extra-cellular conductivities along x respectively, and so on for the other g's. The other details of the model are described in [9].

Clearly, the parameter e is a measure of the difference of anisotropy between the intra- and extra-cellular space, with $e = 0$ when the conductivity anisotropy is the same in both media, i.e. $g_{ex}/g_{ey} = g_{ix}/g_{iy}$. In that last situation, the second PDE becomes independent from the first one and the trans-membrane potential ϕ is enough to describe the electrical potential in the tissue. In the myocardial tissue, $g_{ix}/g_{iy} = 10$ and $g_{ex}/g_{ey} = 5/2$ which give a typical value of $e = 0.75$. Note that, in this model, the myocardial fibers are aligned with the x-axis while the y-axis is a transverse direction with a smaller propagation rate. In the model (1)-(3), the variables x and y are scaled with characteristic lengths λ_x and λ_y, respectively. Unless $e = 0.75$, it can only be ensured that either a) $g_{ix}/g_{iy} = 10$ or b) $g_{ex}/g_{ey} = 5/2$ but not both, assuming a typical value of $\alpha = 1.0$. Cases (a) and (b) give respectively aspect ratios of

$$k_a = \frac{\lambda_x}{\lambda_y} = \sqrt{5(2-e)} \quad \text{and} \quad k_b = \frac{\lambda_x}{\lambda_y} = \sqrt{\frac{5(2-e)}{4(1-e)}}. \tag{4}$$

Typical values of k_a and k_b for the values of e commonly used in the simulations are given in Table 1. For $e = 0$, the "primary" anisotropy of the propagated waves is present (i.e. $k_a \neq 1$ or $k_b \neq 1$), while the "secondary" anisotropy enforcing the use of a second potential ψ does not appear.

2. Finite Element Method

The Eq. (1)-(3) are discretized by first converting the PDEs into variational forms with the second order terms integrated by parts. Continuous linear finite element on triangular meshes are used. The time derivatives

are handled with the fully implicit second order Gear finite difference scheme. This amounts to look for a solution $(\phi_h^{n+1}, \psi_h^{n+1}, v_h^{n+1})$ at time t_{n+1} such that

$$\int_\Omega \frac{3/2\phi_h^{n+1} - 2\phi_h^n + 1/2\phi_h^{n-1}}{\Delta t}\,\theta_h\,dx + \int_\Omega \nabla\phi_h^{n+1}\cdot\nabla\theta_h\,dx = \frac{1}{\epsilon}\int_\Omega f(\phi_h^{n+1}, v_h^{n+1})\,\theta_h\,dx - c_1\int_\Omega \frac{\partial\psi_h^{n+1}}{\partial x}\,\frac{\partial\theta_h}{\partial x}\,dx \quad (5)$$

$$\int_\Omega (D\nabla\psi_h^{n+1})\cdot\nabla\eta_h\,dx = -c_2\int_\Omega \frac{\partial\phi_h^{n+1}}{\partial x}\,\frac{\partial\eta_h}{\partial x}\,dx \quad (6)$$

$$\int_\Omega \frac{3/2v_h^{n+1} - 2v_h^n + 1/2v_h^{n-1}}{\Delta t}\,u_h\,dx = \epsilon\int_\Omega (\phi_h^{n+1} + \beta - \gamma v_h^{n+1})\,u_h\,dx \quad (7)$$

for all continuous piecewise linear functions (θ_h, η_h, u_h) defined on a given triangular mesh. Note that c_1 and c_2 are constants, and D is a diagonal tensor derived from the Eq. (1)-(3).

The resulting nonlinear system is solved with a Newton-GMRES method. The lack of time derivative in Eq. (2) makes the system stiff and strongly coupled, enforcing the introduction of a relaxation method in the usual explicit finite difference methods used for bidomain models [7]. We did not have to use any relaxation method as our implicit Gear scheme and the Newton-GMRES solver naturally resolve the stiffness of the system.

3. Numerical Results

We will present a single test case showing the efficiency of our method in capturing the dynamical evolution of electrophysiological waves in a media with a secondary conduction anisotropy. A general strategy to obtain spiral wave solutions is to start from a truncated asymmetric planar wave in ϕ, go through between 5000 and 10000 time steps of transient solutions before the spiral wave appears and enters its meandering pattern. The spiral tip must be (re)centered in the domain during time stepping to ensure the symmetry of the meandering pattern.

The Figure 1 shows a spiral wave computed on a square domain with a uniform mesh with 300x300 squares, each splitted in two triangular elements. An uniform mesh is used to mimic the behavior of finite difference methods commonly used for bidomain models. A warning should be made, nevertheless, concerning the symmetry breaking induced by cutting each square in two triangles instead of four with an extra node added at the center of the square. The loss of symmetry of the mesh may destroy the symmetry of the solution or of the spiral tip trajectory. For the test case shown, one could verify that our solution and its spiral tip trajectory are similar to the ones obtained by Roth [7], using the same grid resolution. In our case, of course, the uniform grid does not have as many symmetries.

The figure 2 on the left shows the same solution but rescaled using k_a for $e = 0.9$. Clearly, the picture shows a dominant conduction along the fibers.

The same test case has been redone but on a circular disk of radius 30 with a mesh of randomly distributed triangles of almost identical size. The results are shown on Fig. 2 on the right. The spiral looks like the one obtained on the uniform mesh. Moreover, the shape of the domain boundary does not have a noticeable impact, at least to first order, on the evolution of the spiral, provided the spiral tip is centered in the domain. A detailed view of the mesh and the solution close to the spiral tip on both meshes can be seen on Fig. 3. The spatial resolution is almost the same on both meshes, giving rise to similar solutions. The quality of the solutions on both meshes is confirmed by identical spiral tip trajectories, as seen on Fig. 4. The spiral tip trajectories are usually very sensitive to insufficient grid resolution or grid asymmetry. We have noticed that an average of 5 to 10 nodes along the transverse direction in regions with a sharp gradient of the solution is enough to capture the right dynamical behavior of the spiral tip using unstructured mesh methods.

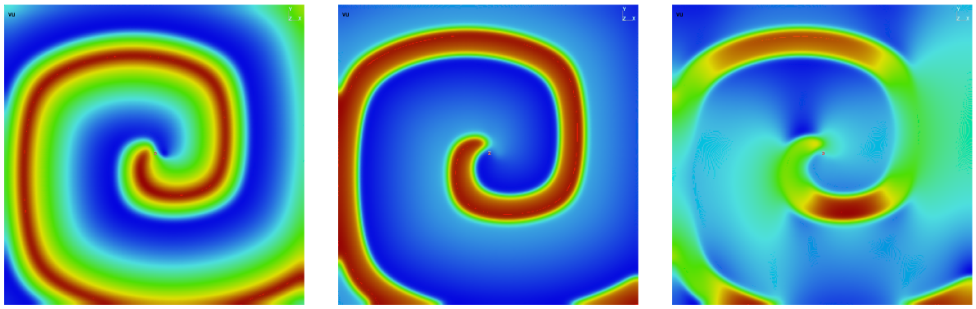

v ϕ ψ

FIGURE 1. Bidomain solution with $\epsilon = 0.2$, $e = 0.9$, $\beta = 0.8$, domain $[-30, 30]^2$, mesh 300x300x2, 10^5 time steps

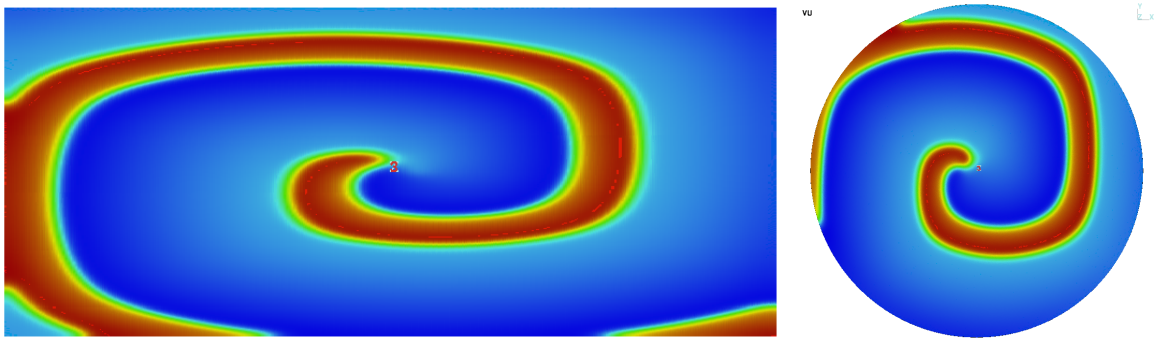

FIGURE 2. Trans-membrane potential ϕ for the solution of Fig. 1, rescaled with $k_a = \frac{\lambda_x}{\lambda_y} = 2.35$ (left) or computed on a disk of radius 30 with an unstructured mesh composed of 195214 triangles (right)

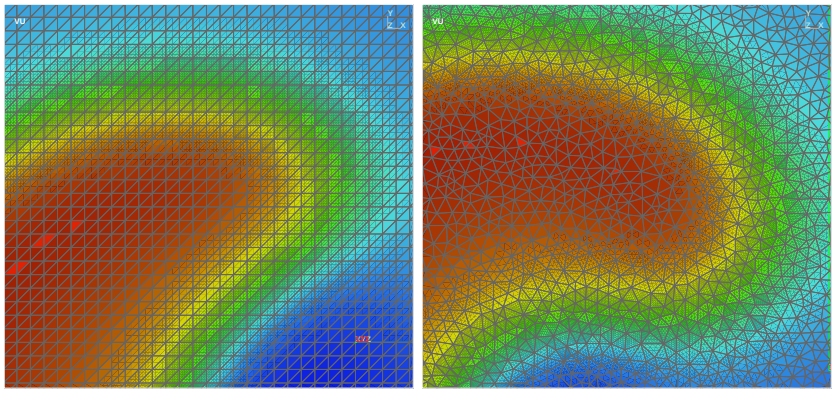

FIGURE 3. Zoom of the mesh superposed with the variable ϕ in the vicinity of the tip of the spiral for the solution of Fig. 1, on an uniform mesh over the square (left) or on an unstructured mesh over the disk (right) (Note: Solutions at different times.)

The authors are thankful to Prof. Victor G. LeBlanc from the University of Ottawa for fruitful discussions during the course of this work.

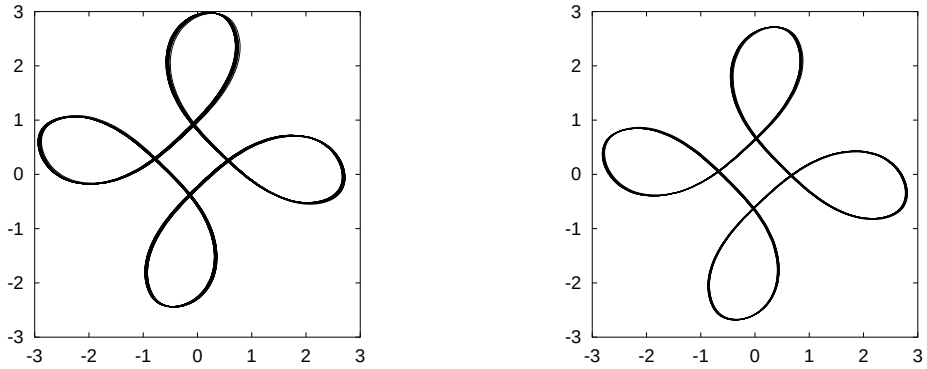

FIGURE 4. Trajectory of the tip of the spiral for the solution of Fig. 1, on an uniform mesh over the square (left) or on an unstructured mesh over the disk (right)

REFERENCES

[1] J. Keener and J. Sneyd. *Mathematical Physiology*. Springer-Verlag, 1998.
[2] N.F. Otani. Computer modeling in cardiac electrophysiology. *J. Comp. Phys.*, 161:21–34, 2000.
[3] D. Barkley. Euclidean symmetry and the dynamics of spiral waves. *Phys. Rev. Lett.*, 72:165–167, 1994.
[4] M. Golubitsky, V.G. LeBlanc and I. Melbourne. Meandering of the spiral tip: An alternative approach. *J. Nonlinear Sci.*, 7:557–586, 1997.
[5] V.S. Zykov and S.C. Müller. Spiral waves on circular and spherical domains of excitable medium. *Physica D*, 97:322–332, 1996.
[6] J. Gomatam and F. Amdjadi. Reaction-diffusion equations on a sphere: Mendering of spiral waves. *Physical Review E*, 56:3913–3919, 1997.
[7] B.J. Roth. Mendering of spiral waves in anisotropic cardiac tissue. *Physica D*, 150:127–136, 2001.
[8] D.M. Harrild and C.S. Henriquez. A finite volume model of cardiac propagation. *Annals Biomed. Eng.*, 25:315–334, 1997.
[9] B.J. Roth. Approximate analytical solutions to the bidomain equations with unequal anisotropy ratio. *Physical Review E*, 55:1819–1826, 1997.